IEEE Access
Multidisciplinary | Rapid Review | Open Access Journal

Received May 8, 2021, accepted May 24, 2021, date of publication May 27, 2021, date of current version June 8, 2021.

Digital Object Identifier 10.1109/ACCESS.2021.3084442

A Novel Signal Normalization Approach to Improve the Force Invariant Myoelectric Pattern Recognition of Transradial Amputees

MD. JOHIRUL ISLAM[1,2], SHAMIM AHMAD[3], (Member, IEEE), FAHMIDA HAQUE[4], MAMUN BIN IBNE REAZ[4], (Senior Member, IEEE), MOHAMMAD A. S. BHUIYAN[5], AND MD. REZAUL ISLAM[1]

[1]Department of Electrical and Electronic Engineering, University of Rajshahi, Rajshahi 6205, Bangladesh
[2]Department of Physics, Rajshahi University of Engineering and Technology, Rajshahi 6204, Bangladesh
[3]Department of Computer Science and Engineering, University of Rajshahi, Rajshahi 6205, Bangladesh
[4]Department of Electrical, Electronic and Systems Engineering, Universiti Kebangsaan Malaysia, Bangi 43600, Malaysia
[5]Department of Electrical and Electronics Engineering, Xiamen University Malaysia, Bandar Sunsuria 43900, Malaysia

Corresponding author: Mohammad A. S. Bhuiyan (arifsobhan.bhuiyan@xmu.edu.my)

This work was supported in part by Xiamen University Malaysia under Project XMUMRF/2018-C2/IECE/0002; in part by the Information and Communication Technology Division, Ministry of Posts, Telecommunications and Information Technology, Government of Bangladesh, under Grant 56.00.0000.028.33.098.18-219; and in part by Universiti Kebangsaan Malaysia under Grant GP-2020-K017701, Grant KK-2020-011, and Grant MI-2020-002.

ABSTRACT Variation in the electromyogram pattern recognition (EMG-PR) performance with the muscle contraction force is a key limitation of the available prosthetic hand. To alleviate this problem, we propose a scheme to realize electromyogram signal normalization across channels before feature extraction. The proposed signal normalization scheme is validated over a dataset of nine transradial amputees that includes three force levels with six hand gestures. Moreover, we employ three classifiers, namely, linear discriminant analysis (LDA), support vector machine (SVM) and k-nearest neighbour (KNN), to evaluate the EMG-PR performance. In addition to the signal normalization scheme, we perform nonlinear transformation of the features by using the logarithm function. Both schemes facilitate merging of the muscle activation patterns of different force levels. The experimental results indicate that the force invariant EMG-PR performance (F1 score of at least 3.24% to 4.34%) of the proposed schemes is significantly enhanced compared to that obtained in recent studies. Therefore, we recommend using these features along with the proposed signal normalization scheme and nonlinear transformation of the features to improve the force invariant EMG-PR performance. The proposed feature extraction method achieves the highest F1 score of 91.28%, 91.39% and 90.56% when using the LDA, SVM and KNN classifiers, respectively.

INDEX TERMS EMG pattern recognition, force invariant features, muscle activation pattern, signal normalization.

I. INTRODUCTION

In recent decades, researchers have focused on surface electromyography (EMG) techniques to realize myoelectric pattern recognition because such techniques can ensure painless and noninvasive detection [1]–[3]. Moreover, the associated data acquisition is simple, the frequency spectrum of the EMG signal is wide (20 Hz to 500 Hz), and the signal carries more information than force myograms and mechanomyograms [4], [5]. However, the previously developed prosthetic hands that adopted the EMG signal strength exhibited a limited number of degrees of freedom (DOFs). Further, researchers have attempted to overcome the problem of limited DOFs by using the EMG-PR-based technique [6]–[8]. In the EMG-PR-based approach, multiple features are extracted from the EMG signal, and the intended hand gestures are predicted using a classifier. Thus, higher DOFs can be achieved for upper-limb prostheses [9]. However, certain critical factors affect the EMG-PR performance, including variation in the muscle contraction force [10]–[13], electrode position shift [14]–[16], hand orientation [17], [18], limb position [17], [19], [20] and

The associate editor coordinating the review of this manuscript and approving it for publication was Alberto Botter.

non-stationarity of the EMG signal [21]. Among these factors, the variation in the muscle contraction force for a specific gesture occurs frequently in our daily activities. The EMG signal amplitude and frequency-domain characteristics change when the contraction force of a respective muscle or group of muscles involved in the particular gesture is varied [22], [23]. Two techniques, frequency summation and multiple fibre summation, are involved in this force variation. In the frequency summation and multiple fibre summation techniques, the action potential sending rate and strength of the action potential from the central nervous system vary, respectively [24]. Therefore, through these physiological changes, the features of EMG signals can be changed with variations in the muscle contraction force.

Tkach *et al.* [25] observed that the EMG-PR performance of time-domain features degrades when the system is tested for the same gesture having different force levels. Furthermore, Scheme and Englehart [26] investigated the impact of the variation in muscle contraction force on the EMG-PR performance. To investigate this aspect, the researchers collected EMG signals with a force variation of 20% to 80% of the maximum voluntary contraction (MVC) in intervals of 10%. Moreover, the authors noted a 55% degradation in the EMG-PR performance when the LDA classifier was tested for unknown force levels. It was suggested that training the classifier with all force levels could help achieve an enhanced EMG-PR performance of 84%. However, prosthetic hand users expect the highest EMG-PR performance in nearly all scenarios, and thus, the performance level should be more than 90% [26]. To achieve the minimum satisfactory performance, Hua *et al.* [27] introduced multitask learning (MTL) to simultaneously recognize gestures and force levels. The authors indicated that the combination of frequency-domain features and convolutional neural networks (CNNs) was more appropriate than amplitude-based features. When frequency-domain features were used, an EMG-PR performance of 95% was achieved. However, in this study, multiple force levels were used to train the CNN. Consequently, the training time was considerable, and the training could not be accomplished using low-cost hardware [11], [28]. Subsequently, He *et al.* [11] proposed a force invariant feature extraction method based on the frequency-domain features normalized across channels. A satisfactory force invariant EMG pattern recognition of 91% was achieved using the LDA classifier. However, the major constraint is that the authors use a specific electrode position on the forearm, which is very tough to ensure for all amputees due to a small stump length. Thereafter, Al-Timemy *et al.* [10] attempted to ensure a satisfactory EMG-PR performance for nine transradial amputees. The authors introduced a new feature extraction method known as time-dependent power spectrum descriptors (TDPSD), which could achieve an EMG-PR performance of nearly 90% when the LDA classifier was trained for all force levels. However, the force invariant EMG-PR performance of amputees is low due to their small stump with a deformed muscle structure [29], [30]. Therefore, it is challenging to improve the force invariant EMG-PR performance for transradial amputees.

In this context, we attempt to enhance the force invariant EMG-PR performance of transradial amputees. To do so, we propose a scheme to normalize the EMG signal across channels before the feature extraction method. The signal normalization scheme is aimed at alleviating the problem of amplitude variation with the variation in the muscle contraction force. The proposed signal normalization scheme is effective for balancing the forces in the raw EMG signal and extracted features since the muscle activation pattern across the channels is unique for each gesture and remains constant with forces except for the strength of the EMG signal [11].

Notably, although the abovementioned studies were aimed at enhancing the EMG-PR performance by introducing more efficient force invariant features, to the best of our knowledge, none of the existing studies have attempted to balance the original EMG signal with the variation in the muscle force levels, thereby balancing the forces for each amplitude-based feature. The proposed signal normalization scheme can significantly enhance the force invariant EMG-PR performance in terms of the accuracy sensitivity, specificity, precision and F1 score. Furthermore, we investigate the impact of nonlinear transformation (logarithm) on the signal normalized features since it enhances the separation margin among the gestures [10], [36]. Therefore, we establish a feature extraction method that employs the proposed signal normalization scheme and nonlinear transformation of features. The EMG-PR performance of the recommended feature extraction method is compared with five existing feature extraction methods. The experimental results (Section III) indicate that the proposed feature extraction method can achieve the highest EMG-PR performance in terms of all the performance evaluation parameters. Furthermore, we consider three widely used classifiers, i.e., LDA, SVM, and KNN, to evaluate and validate our experimental results. These classifiers are selected as they incur a low computational cost and can achieve a reasonable EMG-PR performance [11], [31]–[33]. In addition, the experimental outcomes are validated statistically through Bonferroni-corrected analysis of variance (ANOVA).

The remaining paper is structured as follows. Section II describes the EMG datasets of transradial amputees, the proposed EMG signal normalization scheme, the feature extraction method, and the EMG-PR method. Section III presents the impact of the proposed signal normalization scheme on the raw EMG signal, the muscle activation patterns of different gestures and a comparison and evaluation of the force invariant EMG-PR performance. Section IV investigates the reasons behind the improved EMG-PR performance, and Section V summarizes the overall experimental results.

II. METHODOLOGY

A. DESCRIPTION OF THE EMG DATASET

In this research, we collect the EMG dataset of transradial amputees from [10]. The dataset is also publicly

available on the Khushaba website (www.rami-khushaba.com/ electromyogram-emg-repository.html). The dataset involves the information of seven transradial amputees (TR1-TR7) and two congenital amputees (CG1-CG2). Each amputee performed six hand gestures, including thumb flexion, index flexion, fine pinch, tripod grip, hook grip (hook or snap) and spherical grip (power). In general, it is challenging for an amputee to perform an imaginary gesture. In the dataset formulation, the amputees overcame this challenge with the assistance of another intact hand. Additionally, LabVIEW (National Instruments, USA) software was used to observe the EMG signal on the screen and confirm the response. The amputees performed each hand gesture with three force levels, specifically, low, medium and high. Additionally, the amputees performed every gesture five to eight times (also known as trials) with a variable duration of eight to twelve seconds. Data were collected using a custom EMG data acquisition system, in which the EMG signal was sampled at 2000 Hz. Furthermore, differential EMG signal electrode pairs were placed around the residual forearm with the common electrode placed on the elbow joint.

B. THE PROPOSED EMG SIGNAL NORMALIZATION SCHEME

The EMG signal is stochastic in nature. The amplitude and frequency-domain characteristics of the EMG signal vary with the muscle contraction force [24]. He *et al.* [11] showed that every gesture follows a unique muscle activation pattern (MAP) across channels, which is unique for every gesture. Additionally, this MAP for every gesture does not change with the variation in the force, except for the amplitude. Therefore, the MAP is a stable feature that can be utilized to design a force invariant EMG-PR system. In this research, we attempt to alleviate the problem of signal amplitude variation with the force variation. Therefore, we normalize the multichannel EMG signal for a current window according to the root mean square (RMS) value as defined in (1). The mathematical formula is as follows:

$$Normalized\ EMG\ Signal_j = \frac{X_j}{\sqrt{\frac{1}{MN}\sum_{j=0}^{M-1}\sum_{i=0}^{N-1} x_{j,i}^2}} \tag{1}$$

where j and i present the channel and discrete sample values of sizes M and N (window size), respectively, and X_j denotes the j^{th} EMG channel of a window.

C. FEATURE EXTRACTION

The multichannel EMG signal is normalized across channels for each analysis window, as described in Section II-B. Next, the seven time-domain features and correlation coefficients are extracted. The features are as follows:

The mean value (MV), also known as the mean absolute value, reflects the signal strength of the EMG signal. The MV can be defined as [34]

$$MV = \frac{1}{N}\sum_{i=0}^{N-1} |x[i]| \tag{2}$$

where $x[i]$ is the discrete EMG signal of window size N.

The zero-order power spectrum (P_0) indicates the total power in the frequency domain. P_0 can be derived directly from the discrete time-domain signal by using the Parseval theorem.

$$P_0 = \sum_{i=0}^{N-1} [x[i]]^2 = \frac{1}{N}\sum_{k=0}^{N-1} [X[k]X^*[k]] = \sum_{k=0}^{N-1} P[k] \tag{3}$$

where $P[k]$ is the power spectrum, and $X^*[k]$ is the complex conjugate of $X[k]$ with a frequency index of k.

The second-, fourth- and sixth-order power spectra (P2, P4 and P6, respectively) are considered to correspond to the signal power according to Hjorth *et al.* [35]. The higher-order signal powers can be mathematically defined using the differentiation property of the discrete time-domain signal.

$$P_2 = \sum_{k=0}^{N-1} k^2 P[k] = \frac{1}{N}\sum_{k=0}^{N-1} [kX[k]]^2 = \sum_{i=0}^{N-1} [\Delta x[i]]^2 \tag{4}$$

$$P_4 = \sum_{k=0}^{N-1} k^4 P[k] = \frac{1}{N}\sum_{k=0}^{N-1} [k^2 X[k]]^2 = \sum_{i=0}^{N-1} [\Delta^2 x[i]]^2 \tag{5}$$

$$P_6 = \sum_{k=0}^{N-1} k^6 P[k] = \frac{1}{N}\sum_{k=0}^{N-1} [k^3 X[k]]^2 = \sum_{i=0}^{N-1} [\Delta^3 x[i]]^2 \tag{6}$$

The odd-order power spectra are not considered due to the zero value.

The first- and second-order average amplitude changes (AC_1 and AC_2, respectively) correspond to the average amplitude change, which indicates the indirect frequency information [34].

$$AC_1 = \frac{1}{N-1}\sum_{i=0}^{N-1} |\Delta x| \tag{7}$$

$$AC_2 = \frac{1}{N-2}\sum_{i=0}^{N-1} |\Delta^2 x| \tag{8}$$

Subsequently, the abovementioned seven features are nonlinearly transformed through a logarithmic function to maximize the margin among the gestures, with a focus on the low amplitude values [10], [36]. The nonlinear mean value, zero-order power spectrum, second-order power spectrum, fourth-order power spectrum, sixth-order power spectrum, first-order average amplitude change and second-order average amplitude change are denoted as NLMV, NLP_0, NLP_2, NLP_4, NLP_6, $NLAC_1$ and $NLAC_2$, respectively.

The correlation coefficients (CCs) indicate the strength of the similarity for each pair of EMG channels. The CC depends only on the correlation between two signals instead of their signal amplitude change due to the variation in the

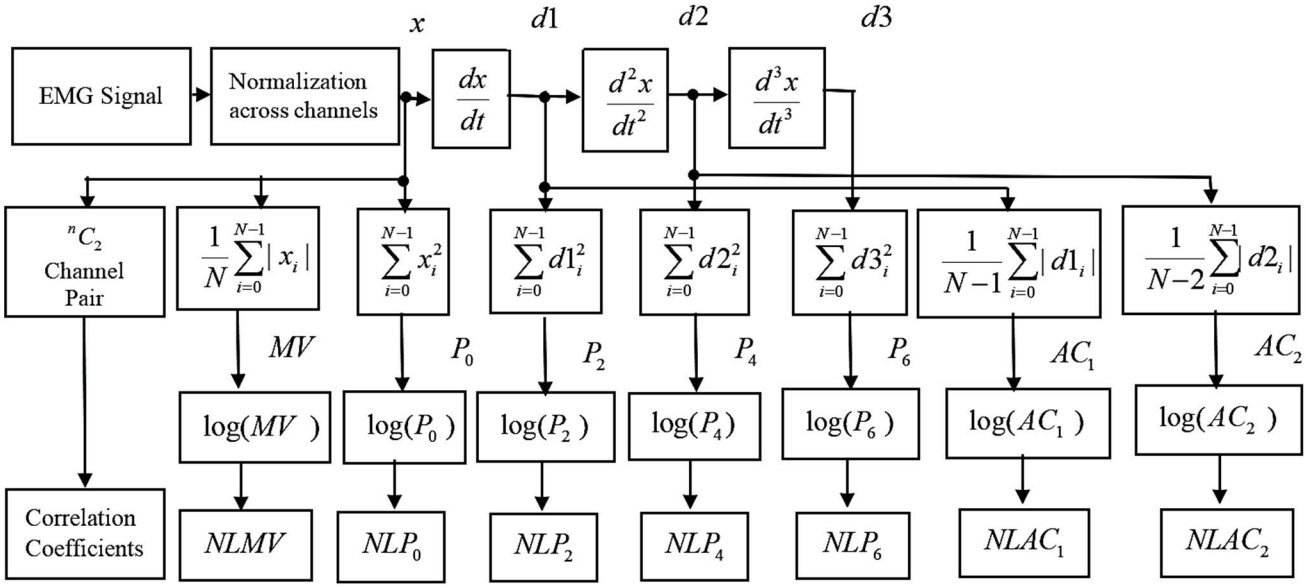

FIGURE 1. Block diagram of feature extraction method.

muscle contraction force. The correlation coefficient $\rho(x, y)$ for channels x and y can be mathematically defined as follows.

$$\rho(x,y) = \frac{Cov(x,y)}{\sigma_x \sigma_y} = \frac{\sum_{i=0}^{N-1}(x_i - \bar{x})(y_i - \bar{y})}{\sqrt{\sum_{i=0}^{N-1}(x_i - \bar{x})^2}\sqrt{\sum_{i=0}^{N-1}(y_i - \bar{y})^2}} \quad (9)$$

where $\bar{x}$ and $\bar{y}$ present the mean of channels x and y for a window size of N, respectively. The entire feature extraction procedure is summarized in Fig. 1.

D. EMG PATTERN RECOGNITION

In this paper, MATLAB 2017a software is used to evaluate the EMG-PR performance. We adopt an overlapped rectangular windowing or segmentation scheme with a window size of 250 ms and 100 ms overlap between successive windows. In this scenario, the EMG-PR system requires $(150 + \tau)$ ms to predict the intended gesture, where τ is the processing time of a classifier. Therefore, the required processing time for the EMG-PR is less than the recommended limit [37]. Furthermore, the movement artefacts [38], high-frequency noise [39] and power line artefacts [40] are removed using multiple digital filters, specifically, a high-pass filter of 20 Hz, low-pass filter of 500 Hz and notch filter of 50 Hz, respectively.

To evaluate and compare the impact of the proposed normalization on the EMG-PR performance, we consider four cases involving seven features with the CC, as described in Section II-C. The case descriptions are as follows:

This feature extraction method includes MV, P_0, P_2, P_4, P_6, AC_1, AC_2 and CC and is termed case A. The proposed signal normalization scheme is not used here.

He *et al.* [11] used a feature normalization scheme across channels. In this feature normalization scheme, each of the considered features (MV, P_0, P_2, P_4, P_6, AC_1, and AC_2) for a current window is normalized according to Euclidean norm across channels. Again, normalized features MV, P_0, P_2, P_4, P_6, AC_1, and AC_2 along with the original CC, termed case B.

In this research, we propose a scheme involving EMG signal normalization across channels, as described in Section II-B. This framework is used in case C with the considered features (MV, P_0, P_2, P_4, P_6, AC_1, AC_2 and CC).

In case D, we employ nonlinear transformation (logarithm) in addition to the case C features, except CC. Hence, the feature set includes NLMV, NLP_0, NLP_2, NLP_4, NLP_6, $NLAC_1$, $NLAC_2$ and CC.

In all the cases, the extracted features generate an 84-dimensional feature space (7 features $\times$ 8 channels + ${}^8C_2$ CC $= 56 + 28 = 84$). However, spectral regression discriminant analysis (SRDA) reduces the high-dimensional feature space to 5 (total number of gestures $-1 =$ 6-1 $= 5$) [41]. To evaluate the EMG-PR performance of the considered feature extraction method, we use three classifiers: LDA with a quadratic function [42], [43], SVM with a Gaussian radian basis kernel function [44], [44] and KNN with three neighbours [45], [46]. In this study, we consider five trials with eight channels placed around the forearm since these channels are variable in this dataset. Moreover, we use four trials as the training set and the remaining trial as the testing set. The training and testing sets are changed five times to ensure that every trial is used as a testing set. In the training and testing sessions, the number of samples is equal to the product of the force levels, trials, gestures and number of samples per trial. Furthermore, the data overfitting problem is carefully addressed, as confirmed by the negligible difference in the performance between the training and

testing sessions. Finally, the EMG-PR performance is evaluated through the accuracy, sensitivity, specificity, precision, and F1 score [47], [48]. These performance evaluation parameters define the ability to distinguish true positive and true negative gestures. Further, the F1 score is evaluated based on both sensitivity and precision to more accurately identify the true positive gestures. These parameters can be measured as follows:

$$Accuracy = \frac{TP + TN}{TP + TN + FP + FN} \tag{10}$$

$$Sensitivity = \frac{TP}{TP + FN} \tag{11}$$

$$Specificity = \frac{TN}{TN + FP} \tag{12}$$

$$Precision = \frac{TP}{TP + FP} \tag{13}$$

$$F1Score = \frac{2 \times Precision \times Sensitivity}{Precision + Sensitivity} \tag{14}$$

where *TP, TN, FP*, and *FN* represent true positive, true negative, false positive, and false negative values, respectively.

E. STATISTICAL TEST

To evaluate the statistical significance between any two feature extraction methods, we perform Bonferroni-corrected ANOVA with a confidence level of 95%. In this study, the amputee-wise EMG-PR performance under three training cases is concatenated to form a 27-dimensional vector (9 amputees $\times$ 3 training-test cases), and Bonferroni-corrected ANOVA is performed. Additionally, the ANOVA findings are discussed in Sections III-E and III-F, with the number of training-testing cases being one.

III. RESULTS

A. IMPACT OF EMG SIGNAL NORMALIZATION ACROSS CHANNELS

The multichannel raw EMG signal with three force levels shown in Fig. 2a indicates that the signal amplitude changes more markedly than the frequency-domain characteristics. Therefore, the EMG signal of the 250 ms window (sampling frequency $\times$ window size $= 2000 \times 0.25 = 500$ samples) is normalized across channels according to the RMS value. The normalized signal is shown in Fig. 2b for all channels with three force levels. Fig. 2b indicates that the EMG signal normalization scheme balances the three forces.

B. MUSCLE ACTIVATION PATTERN

To observe the MAP with three forces, we consider the eight-channel EMG signal of amputee 1 with six hand gestures. Next, a feature (MV) is calculated for a single window, and the features for all forces are scaled between 0 and 1. Finally, the scaled MV values are plotted in a radar plot. Fig. 3 shows the MAP of the six hand gestures with three force levels, with A, B, C and D indicating the four considered cases. Case A in Fig. 3 corresponds to a unique MAP for every gesture, and the strength of the active muscles increases with the increase in the muscle contraction force. Furthermore, a weak EMG signal strength is present at the inactive muscle positions due to propagation of the EMG signal through the skin. The EMG signal strength decays with increasing EMG source separation. Moreover, the MAP is not identical for all force levels for an amputee, although an intact limbed subject produces identical MAPs for all force levels [11], [49]. The possible reasons may be lack of proper training to perform a given gesture and the deformed muscle structure. In addition, Fig. 3 shows that the problem of EMG signal strength variation with the force levels is alleviated when feature normalization (case B) and EMG signal normalization scheme are implemented across channels (case C). In addition, the logarithm transformation of the signal normalized feature (case D) shows improved feature overlapping for the three force levels.

C. FORCE INVARIANT EMG-PR PERFORMANCE WITH A SINGLE TRAINING FORCE

To evaluate the force invariant EMG-PR performance, we train the classifiers with a single force level and test them with all force levels. The average EMG-PR performance and standard deviations across the amputees for different training cases are shown in Table 1. The experimental results shown in Table 1 indicate that the proposed EMG signal normalization scheme used in cases C and D provides better force invariant EMG-PR performance in terms of the accuracy, sensitivity, specificity, precision and F1 score. In addition to the highest EMG-PR performance, cases C and D achieve the lowest coefficient of variation in most cases. Again, it is noted that nonlinear transformation through the logarithm function (case D) significantly contributes to the force invariant EMG-PR performance since the p values (Appendix A, Table 5) are less than 0.012 when case C is compared with case D (except for the F1 score with the KNN classifier ($p = 0.019$)). In this study, the proposed signal normalization scheme with nonlinear transformation (case D) improves the accuracy, sensitivity, specificity, precision and F1 score by 1.45%, 4.35%, 0.89%, 4.13% and 4.34%, respectively, when case D is compared to the existing feature normalization scheme (case B) with the LDA classifier trained at a medium force level. Additionally, the SVM and KNN classifiers follow a trend similar to that of LDA and yield a nearly similar performance enhancement. However, for training with a single force, the LDA classifier achieves the highest F1 score of 77.99% when trained under a medium force level. To demonstrate the significant performance improvement induced by the proposed signal normalization scheme along with nonlinear transformation (case D) compared with cases A and B, we consider the Bonferroni-corrected ANOVA findings for each classifier. The highest p value (Appendix A, Table 5) is less than 0.001 for all cases, which demonstrates that the proposed signal normalization scheme with nonlinear transformation (case D) significantly improves the force invariant performance.

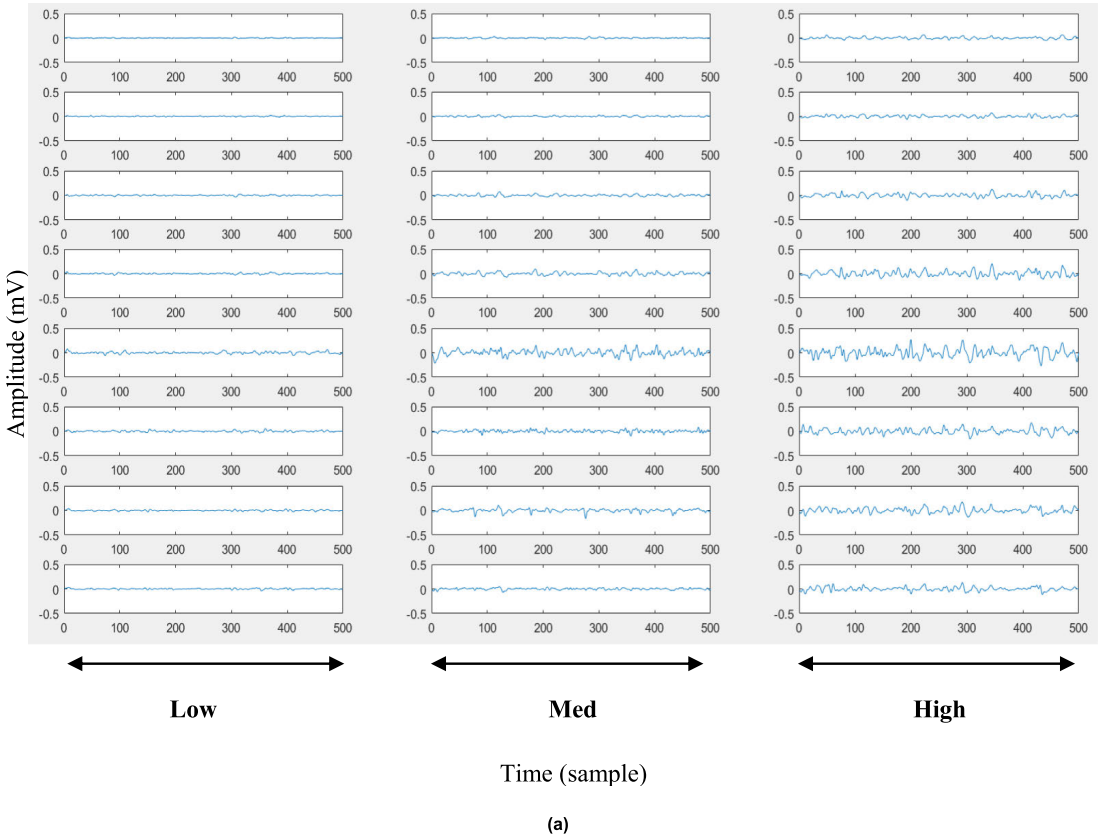

(a)

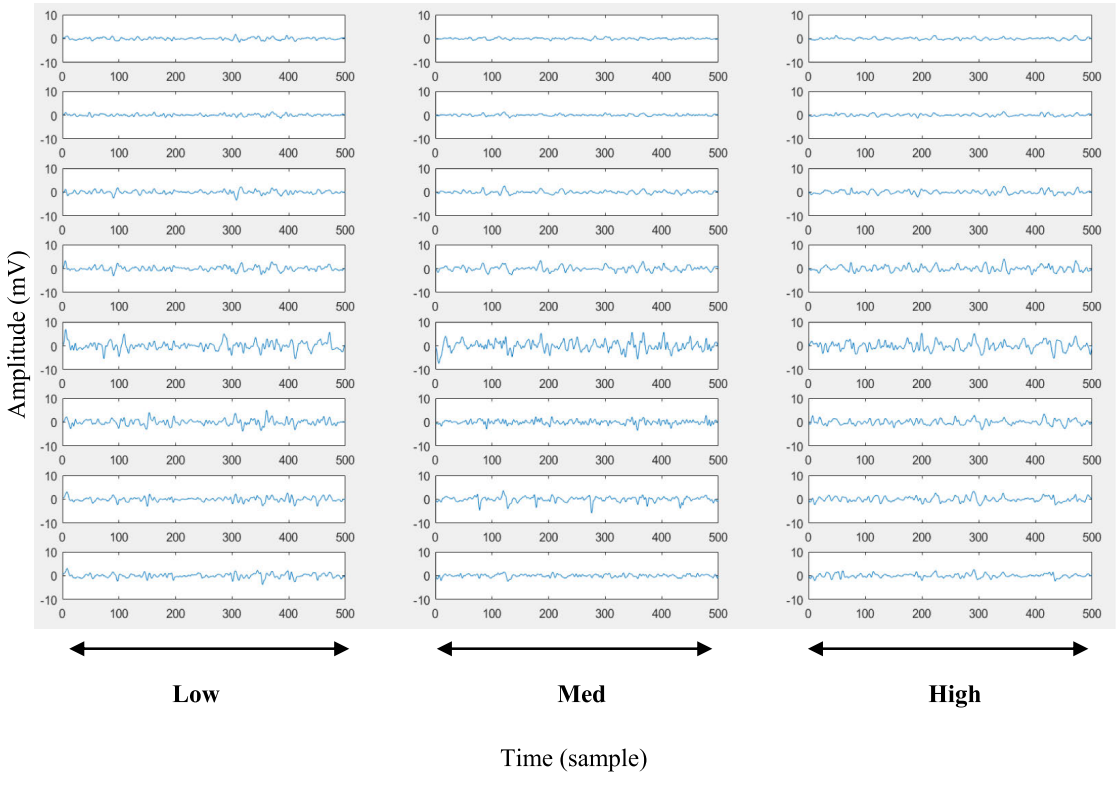

(b)

FIGURE 2. The raw EMG signal where (a) is the original EMG signal and (b) is normalized EMG signal across channels.

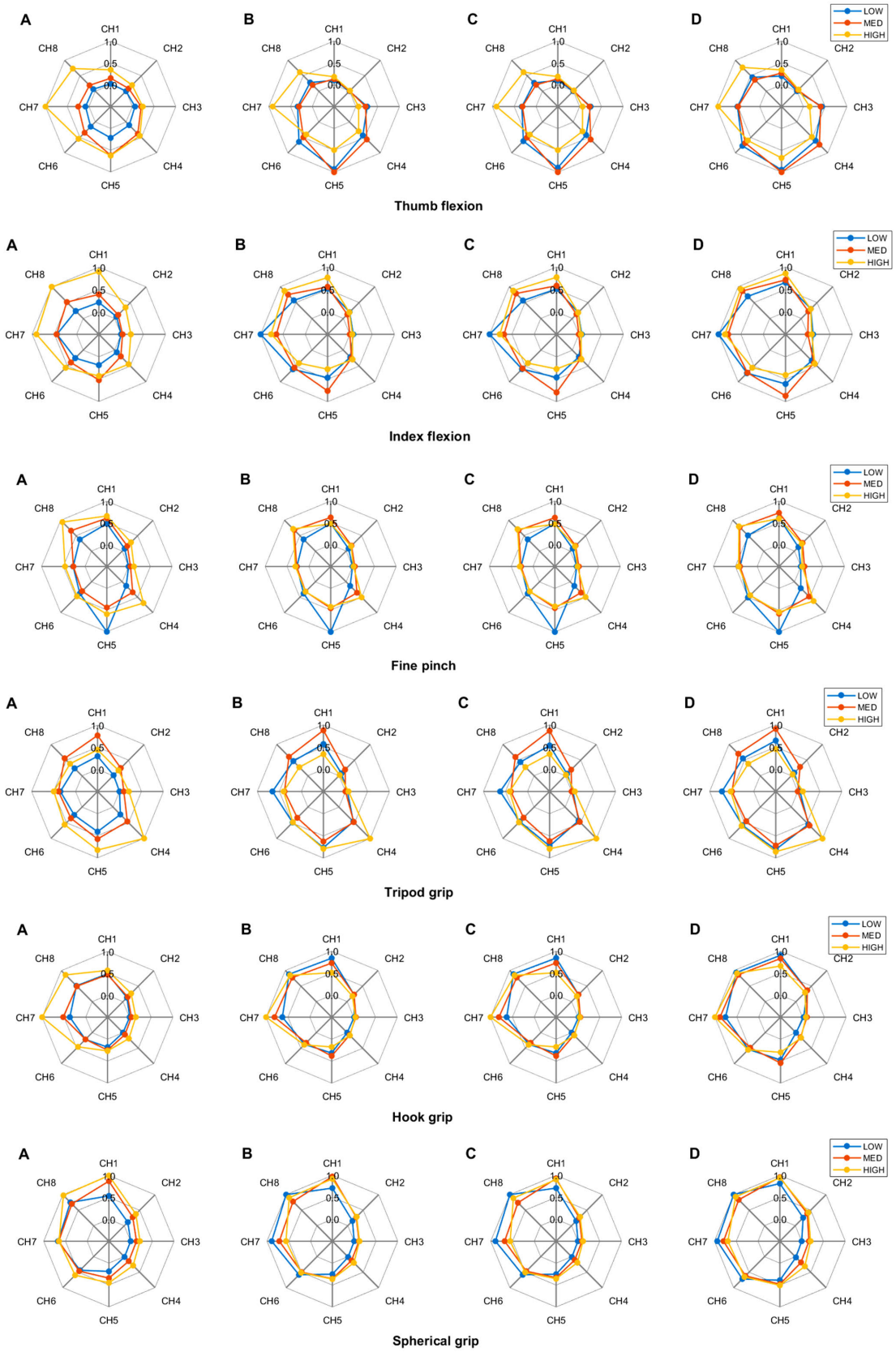

FIGURE 3. The radar plot of six hand gestures for three force levels using MV feature where (A) is the original feature, (B) is feature normalized across channels, (C) is the proposed signal normalized feature and (D) is the proposed signal normalized feature with logarithm transformation.

TABLE 1. The EMG-PR performances where the classifiers are trained with a single force level and tested with all force levels.

	Parameter	Classifier	Case-A	Case-B	Case-C	Case-D
Training with low force	Accuracy	LDA	87.66±2.69	88.72±2.53	89.76±2.56	90.12±2.90
		SVM	87.60±2.70	88.79±2.53	89.91±2.39	90.13±2.64
		KNN	88.52±2.23	88.85±2.48	89.97±2.36	90.00±2.65
	Sensitivity	LDA	62.98±8.07	66.15±7.60	69.29±7.67	70.37±8.71
		SVM	62.79±8.10	66.37±7.59	69.72±7.17	70.39±7.91
		KNN	65.56±6.68	66.55±7.45	69.92±7.08	70.01±7.96
	Specificity	LDA	92.92±1.45	93.45±1.43	94.08±1.39	94.30±1.58
		SVM	92.79±1.50	93.44±1.50	94.12±1.38	94.28±1.46
		KNN	93.28±1.34	93.45±1.45	94.16±1.37	94.20±1.50
	Precision	LDA	71.77±5.84	73.24±4.65	75.92±4.22	77.01±5.04
		SVM	71.18±6.82	71.99±5.29	75.34±4.22	76.31±4.73
		KNN	71.62±5.06	72.10±5.18	75.28±4.11	75.67±4.85
	F1 Score	LDA	62.67±7.43	65.72±7.28	68.96±7.17	70.06±8.31
		SVM	63.00±7.42	66.09±7.44	69.58±6.80	70.27±7.57
		KNN	65.28±6.44	66.24±7.33	69.80±6.76	69.86±7.77
Training with medium force	Accuracy	LDA	90.26±2.01	91.29±2.30	92.23±20.0	92.74±2.01
		SVM	90.27±2.21	91.36±2.24	92.34±2.13	92.69±1.98
		KNN	90.33±2.09	91.34±2.24	92.34±2.12	92.64±1.98
	Sensitivity	LDA	70.79±6.03	73.88±6.89	76.70±6.01	78.23±6.03
		SVM	70.81±6.64	74.09±6.73	77.02±6.40	78.07±5.93
		KNN	70.99±6.28	74.01±6.71	77.01±6.37	77.93±5.95
	Specificity	LDA	94.23±1.25	94.85±1.41	95.43±1.25	95.74±1.23
		SVM	94.22±1.36	94.91±1.37	95.48±1.33	95.71±1.23
		KNN	94.23±1.30	94.88±1.39	95.48±1.33	95.67±1.25
	Precision	LDA	73.89±5.15	76.80±5.64	79.18±5.30	80.93±5.01
		SVM	74.22±5.45	76.99±5.36	79.65±5.30	80.93±4.92
		KNN	74.08±5.02	76.52±5.68	79.46±5.41	80.55±5.02
	F1 Score	LDA	70.68±5.78	73.65±6.78	76.53±5.99	77.99±6.04
		SVM	70.72±6.29	73.93±6.58	76.91±6.28	77.95±5.87
		KNN	70.91±5.90	73.82±6.57	76.92±6.24	77.80±5.89
Training with high force	Accuracy	LDA	88.63±2.52	88.96±2.88	90.12±2.42	90.60±2.40
		SVM	88.56±2.65	88.81±2.99	89.74±2.33	90.47±2.08
		KNN	88.25±2.62	88.80±2.95	89.64±2.59	90.16±2.43
	Sensitivity	LDA	65.89±7.57	66.88±8.64	70.36±7.25	71.81±7.19
		SVM	65.69±7.95	66.44±8.97	69.23±6.99	71.40±6.24
		KNN	64.75±7.86	66.40±8.85	68.93±7.76	70.49±7.30
	Specificity	LDA	93.08±1.45	93.33±1.74	94.01±1.45	94.32±1.43
		SVM	93.04±1.49	93.24±1.80	93.77±1.37	94.23±1.23
		KNN	92.79±1.48	93.19±1.78	93.67±1.54	94.02±1.47
	Precision	LDA	70.80±5.75	71.50±7.31	74.75±5.79	76.14±5.96
		SVM	71.19±5.58	71.04±7.61	73.72±4.93	75.64±5.01
		KNN	70.84±5.63	70.86±7.70	73.65±5.95	74.98±5.75
	F1 Score	LDA	65.29±7.37	66.52±8.50	70.13±7.04	71.28±7.09
		SVM	65.08±7.25	66.09±8.56	69.03±6.43	70.80±5.89
		KNN	64.24±7.37	66.12±8.56	68.83±7.15	70.14±6.93

D. FORCE INVARIANT EMG-PR PERFORMANCE WITH TWO TRAINING FORCES

To improve the force invariant EMG-PR performance, we employ two training forces and test with all force levels. Table 2 shows the average EMG-PR performance across all amputees under the different training cases. The experimental results shown in Table 2 demonstrate that the proposed signal normalization scheme used in cases C and D achieves the highest EMG-PR performance in terms of all performance evaluation parameters, i.e., accuracy, sensitivity, specificity, precision and F1 score. In addition to the highest EMG-PR performance, cases C and D achieve the lowest coefficient

TABLE 2. The EMG-PR performances where classifiers are trained with two force levels and tested with all force levels.

	Parameter	Classifier	Case-A	Case-B	Case-C	Case-D
Training with low and medium forces	Accuracy	LDA	93.14±1.65	93.68±1.92	94.54±1.74	94.98±1.74
		SVM	93.01±1.69	93.62±2.00	94.62±1.66	94.89±1.79
		KNN	93.16±1.81	93.53±1.97	94.48±1.61	94.75±1.75
	Sensitivity	LDA	79.43±4.96	81.04±5.76	83.63±5.22	84.95±5.23
		SVM	79.04±5.07	80.87±5.99	83.86±4.98	84.67±5.38
		KNN	79.49±5.44	80.60±5.91	83.43±4.83	84.26±5.26
	Specificity	LDA	96.00±0.95	96.32±1.06	96.83±0.95	97.10±0.95
		SVM	95.93±0.96	96.28±1.11	96.86±0.91	97.05±0.99
		KNN	95.97±1.08	96.21±1.11	96.76±0.89	96.95±0.98
	Precision	LDA	81.50±4.81	83.19±4.80	85.46±4.46	86.63±4.32
		SVM	81.32±4.60	82.87±5.03	85.55±4.29	86.44±4.42
		KNN	81.00±5.23	82.42±5.20	84.85±4.37	85.70±4.60
	F1 Score	LDA	79.34±4.89	81.04±5.61	83.60±5.12	84.92±5.10
		SVM	79.09±4.98	80.87±5.83	83.82±4.86	84.67±5.19
		KNN	79.37±5.47	80.55±5.80	83.35±4.75	84.20±5.16
Training with low and high forces	Accuracy	LDA	94.53±2.00	95.04±1.78	95.88±1.52	96.13±1.42
		SVM	94.58±2.06	95.09±1.80	95.90±1.48	96.13±1.47
		KNN	94.13±2.23	94.82±1.93	95.61±1.57	95.84±1.54
	Sensitivity	LDA	83.58±5.99	85.13±5.34	87.65±4.55	88.39±4.25
		SVM	83.75±6.17	85.26±5.40	87.69±4.44	88.38±4.40
		KNN	82.38±6.68	84.47±5.80	86.83±4.70	87.52±4.62
	Specificity	LDA	96.75±1.19	97.06±1.05	97.57±0.88	97.72±0.83
		SVM	96.77±1.24	97.07±1.07	97.57±0.87	97.71±0.87
		KNN	96.48±1.37	96.91±1.16	97.39±0.93	97.53±0.91
	Precision	LDA	84.39±6.13	86.06±5.22	88.44±4.61	89.15±4.22
		SVM	84.65±6.33	86.20±5.21	88.52±4.43	89.18±4.33
		KNN	83.29±6.92	85.36±5.73	87.61±4.81	88.23±4.68
	F1 Score	LDA	83.46±6.14	85.05±5.34	87.56±4.61	88.29±4.29
		SVM	83.66±6.28	85.19±5.38	87.63±4.45	88.29±4.43
		KNN	82.28±6.81	84.41±5.79	86.74±4.79	87.41±4.70
Training with medium and high forces	Accuracy	LDA	92.89±1.98	93.57±1.85	94.67±1.87	95.00±1.81
		SVM	92.93±2.01	93.47±1.81	94.55±1.90	94.92±1.75
		KNN	92.61±2.09	93.32±1.94	94.42±1.88	94.70±1.74
	Sensitivity	LDA	78.66±5.93	80.72±5.54	84.02±5.62	85.01±5.44
		SVM	78.79±6.03	80.41±5.42	83.64±5.69	84.76±5.24
		KNN	77.82±6.28	79.95±5.83	83.27±5.63	84.10±5.23
	Specificity	LDA	95.74±1.21	96.23±1.12	96.87±1.09	97.08±1.06
		SVM	95.77±1.22	96.15±1.08	96.78±1.11	97.01±1.02
		KNN	95.57±1.28	96.05±1.17	96.71±1.11	96.88±1.03
	Precision	LDA	81.22±4.86	82.76±4.38	85.80±4.43	86.73±4.50
		SVM	81.65±4.69	82.55±4.13	85.58±4.33	86.60±4.22
		KNN	80.67±5.12	81.99±4.82	85.15±4.47	85.83±4.48
	F1 Score	LDA	78.58±5.69	80.62±5.33	83.94±5.45	84.85±5.40
		SVM	78.75±5.69	80.34±5.14	83.60±5.45	84.61±5.09
		KNN	77.83±5.95	79.87±5.58	83.22±5.39	83.94±5.12

of variation in most cases. Additionally, nonlinear transformation of the signal normalized features through the logarithm function helps significantly enhance the force invariant EMG-PR performance since the obtained p values (Appendix A, Table 6) between cases C and D for each classifier are considerably smaller than 0.001. The proposed signal normalization scheme along with nonlinear transformation (case D) enhances the accuracy, sensitivity, specificity, precision and F1 score compared with those obtained using the existing feature normalization scheme (case B) by 1.09%, 3.26%, 0.66%, 3.09% and 3.24%, respectively, when the LDA classifier is trained under low and high force levels.

TABLE 3. The EMG-PR performances where the classifiers are trained and tested with all force levels.

Parameter	Classifier	Case-A	Case-B	Case-C	Case-D
Accuracy	LDA	95.75±1.55	96.13±1.32	96.80±1.26	97.12±1.21
	SVM	95.89±1.69	96.18±1.42	96.83±1.30	97.15±1.27
	KNN	95.37±1.91	95.86±1.55	96.51±1.47	96.87±1.40
Sensitivity	LDA	87.24±4.66	88.38±3.97	90.41±3.79	91.36±3.64
	SVM	87.66±5.07	88.54±4.26	90.48±3.91	91.45±3.81
	KNN	86.10±5.72	87.57±4.65	89.54±4.41	90.62±4.21
Specificity	LDA	97.49±0.95	97.73±0.79	98.12±0.73	98.31±0.71
	SVM	97.57±1.02	97.75±0.84	98.14±0.76	98.33±0.74
	KNN	97.25±1.16	97.55±0.94	97.95±0.86	98.17±0.82
Precision	LDA	87.87±4.70	89.02±3.89	90.90±3.73	91.74±3.54
	SVM	88.27±5.01	89.16±4.13	91.01±3.78	91.95±3.64
	KNN	86.68±5.71	88.10±4.62	89.99±4.38	91.05±4.09
F1 Score	LDA	87.14±4.74	88.30±4.02	90.35±3.83	91.28±3.66
	SVM	87.59±5.12	88.47±4.28	90.42±3.93	91.39±3.82
	KNN	86.02±5.79	87.48±4.73	89.47±4.46	90.56±4.23

However, the LDA classifier achieves an improved F1 score of 88.29% when the LDA classifier is trained under low and high force levels. Additionally, the SVM and KNN classifiers provide consistent EMG-PR performance similar to that of the LDA. To demonstrate the significant performance enhancement induced by the proposed signal normalization scheme with nonlinear transformation (case D) against cases A and case B, we evaluate the Bonferroni-corrected ANOVA findings for each classifier. The obtained highest p value (Appendix A, Table 6) is less than 0.001 for all cases, which confirms the significant improvement in case D.

E. EMG-PR PERFORMANCE WITH ALL TRAINING FORCES

To further enhance the EMG-PR performance, we train the classifiers with all force levels and test them with all force levels. Table 3 shows the average EMG-PR performance with the standard deviation across all amputees. The experimental results shown in Table 3 imply that the proposed signal normalization scheme used in cases C and D achieves the highest EMG-PR performance in terms of all the performance evaluation parameters, i.e., the accuracy, sensitivity, specificity, precision and F1 score. Additionally, cases C and D correspond to the lowest coefficient of variation in almost all cases. As in the previously described scenarios, the nonlinear transformation of the signal normalized features significantly enhances the EMG-PR performance and achieves the highest p value (Appendix A, Table 7) of 0.005 between cases C and D for all classifiers. Thus, the proposed signal normalization scheme along with the nonlinear transformation (case D) enhances the accuracy, sensitivity, specificity, precision and F1 score compared with those of the existing feature normalization scheme (case B) by 0.99%, 2.98%, 0.58%, 2.72% and 2.98%, respectively, when the LDA classifier is used. In this training case, the LDA classifier achieves an F1 score of 91.28%, and the value for the other two classifiers, SVM and KNN, follow that of the LDA classifier. Finally, we evaluate the ANOVA findings between cases D and A, and D and B for each classifier. The highest p value (Appendix A, Table 7) is less than 0.001, which demonstrates that the proposed signal normalization scheme with nonlinear transformation (case D) can significantly enhance the performance.

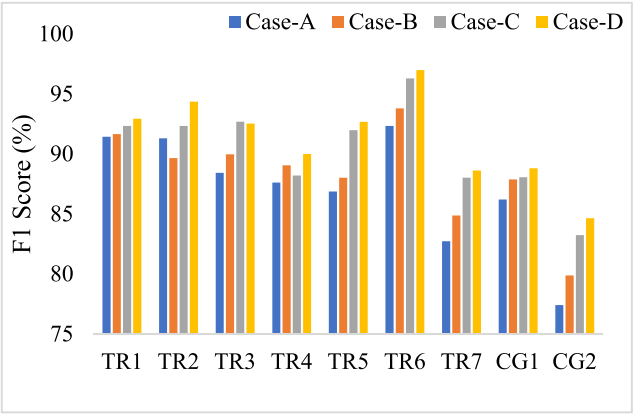

FIGURE 4. The amputee-wise EMG-PR performances using LDA classifier.

The amputee-wise EMG-PR performance (F1 score) under the four cases (cases A–D) when using the LDA classifier is shown in Fig. 4, where the classifier is trained and tested under all force levels. Fig. 4 indicates that the nonlinear (logarithm) transformation of the proposed signal normalized features (case D) corresponds to the highest EMG-PR performance across all amputees except for TR3, for which the proposed signal normalization scheme (case C) achieves the highest performance. The two other classifiers, SVM and

TABLE 4. The comparison of EMG-PR performance where the classifiers are trained and tested with all force levels.

Parameter	Classifier	AR-RMS	TDF	Wavelet	TDPSD	TSD	Case-D
Accuracy	LDA	95.07±1.84	94.80±2.36	95.58±1.81	96.03±1.69	96.56±1.19	97.12±1.21
	SVM	95.10±1.92	94.90±2.39	95.52±1.87	96.14±1.79	96.60±1.20	97.15±1.27
	KNN	94.37±2.21	94.30±2.68	95.00±2.13	95.69±2.01	96.25±1.37	96.87±1.4
Sensitivity	LDA	85.21±5.52	84.39±7.09	86.75±5.44	88.10±5.08	89.68±3.57	91.36±3.64
	SVM	85.31±5.77	84.70±7.16	86.57±5.61	88.42±5.37	89.81±3.61	91.45±3.81
	KNN	83.12±6.64	82.90±8.04	85.00±6.40	87.08±6.02	88.75±4.12	90.62±4.21
Specificity	LDA	97.08±1.09	96.91±1.43	97.39±1.07	97.67±0.98	97.99±0.68	98.31±0.71
	SVM	97.10±1.14	96.97±1.43	97.36±1.11	97.73±1.04	98.02±0.69	98.33±0.74
	KNN	96.64±1.34	96.57±1.64	97.03±1.28	97.46±1.17	97.80±0.80	98.17±0.82
Precision	LDA	85.79±5.50	84.94±7.14	87.23±5.38	88.73±5.07	90.28±3.43	91.74±3.54
	SVM	85.88±5.66	85.29±7.01	87.07±5.56	89.06±5.26	90.40±3.45	91.95±3.64
	KNN	83.53±6.69	83.34±8.09	85.39±6.42	87.65±5.98	89.31±4.04	91.05±4.09
F1 Score	LDA	85.11±5.60	84.24±7.15	86.63±5.47	87.96±5.10	89.62±3.59	91.28±3.66
	SVM	85.25±5.80	84.61±7.16	86.49±5.61	88.33±5.39	89.76±3.62	91.39±3.82
	KNN	83.00±6.75	82.76±8.13	84.89±6.46	86.97±6.06	88.70±4.16	90.56±4.23

KNN, also provide an EMG-PR performance similar to that of LDA.

F. COMPARISON OF THE EMG-PR PERFORMANCE

We compare the proposed signal normalization scheme with nonlinear transformation of features (case D) with five recently reported models, namely, temporal-spatial descriptors (TSD) [31], TDPSD [10], Symmlet-8 wavelet-based features with five levels of decomposition (wavelet) [50], six time-domain features (TDF) [51] and six-order autoregressive coefficients with RMS values (AR-RMS) [52]. A comparison of the average EMG-PR performance with the standard deviation across nine amputees is shown in Table 4. The proposed signal normalization scheme with nonlinear transformation (case D) achieves the highest EMG-PR performance in terms of the accuracy, sensitivity, specificity, precision and F1 score. When comparing case D with each of the existing feature extraction methods, the highest p value, as shown in Appendix A, Table 8 (ANOVA), is 0.009; this result strongly suggests that the proposed signal normalization scheme with nonlinear transformation (case D) significantly improves the EMG-PR performance compared with that of the considered models. In particular, case D achieves the highest performance, and TSD achieves the second-highest EMG-PR performance.

The amputee-wise EMG-PR performance (F1 score) obtained using the six feature extraction methods is shown in Fig. 5, with the LDA classifier trained and tested under all force levels. Fig. 5 indicates that the proposed signal normalization scheme with nonlinear (logarithm) transformation (case D) achieves the highest EMG-PR performance for most of the amputees. In TR6 and TR7, the proposed case D achieves the second-highest EMG-PR performance.

IV. DISCUSSION

In our daily life, we employ various muscle force levels for each gesture, depending on the activities. However, the variation in the muscle force levels is considered a vital limiting factor leading to unsatisfactory EMG-PR performance of myoelectric prosthetic hands [10]–[13]. The reason for the degraded EMG-PR performance is that when the muscle force level is changed, the corresponding amplitude and frequency characteristics of the EMG signal also change depending on the physiology of the muscle [22]. The EMG signal amplitude changes more dominantly than the frequency-domain characteristics [11], [27].

In this study, the proposed EMG signal normalization scheme aims to balance the signal amplitude for different force levels. The proposed signal normalization scheme is

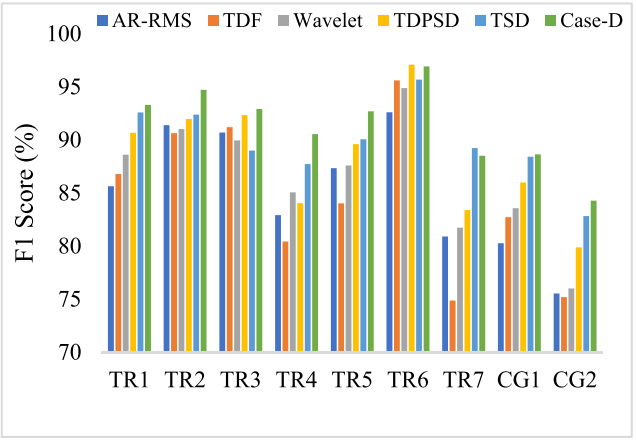

FIGURE 5. The amputee-wise EMG-PR performances using LDA classifier.

highly effective since the MAP is unique for each gesture except in terms of the signal strength, which changes with the muscle force levels [11]. Thus, when the EMG signal is normalized by the RMS value across the channels, all the force levels are balanced through the higher amplification of the low-force EMG signal than the high-force EMG signal. The advantages of the proposed signal normalization scheme are that it provides a consistent performance enhancement in terms of the accuracy, sensitivity, specificity, precision and F1 score, is effective for all transradial amputees with different stump lengths and does not require individual normalization of each feature. In addition, nonlinear transformation of the signal normalized features (case D) facilitates enhancement of the separation margin among the gestures. Thus, nonlinear transformation also significantly contributes to the force invariant EMG-PR performance. The proposed signal normalization scheme with nonlinear transformation of the features (case D) improves the force invariant EMG-PR performance (F1 score when using the LDA) by 3.24% to 4.34% compared to the feature normalization scheme. Therefore, the proposed signal normalization scheme with nonlinear scaling of features represents the best option for the force invariant EMG-PR recognition of amputees, in contrast to using a feature normalization scheme [11]. Therefore, the proposed signal normalization scheme with nonlinear transformation of the features (case D) achieves the highest F1 score (LDA, 91.28%; SVM, 91.39%; KNN, 90.56%), satisfying the criterion of the lowest EMG-PR performance [26]. Specifically, the proposed signal normalization scheme provides a consistent EMG-PR performance even when using different classifiers and overcomes the high classifier dependence of phasor-representation-based force invariant feature extraction methods [12]. In addition, the achieved EMG-PR performance is much better than that with the TDPSD, TSD and recently proposed fractal feature set [10], [31], [53]. Further, compared to the recommended method, traditional feature extraction methods, namely, AR-RMS, TDF and wavelet, provide very poor force invariant EMG-PR performance [50]–[52]. Therefore, these feature extraction methods should be modified for use in this context.

In this study, it is also observed that the MAP of transradial amputees does not follow a trend with the force levels similar to that of intact limbed subjects [11]. The possible reasons for the irregular MAP in the case of amputees may be the deformed muscle structure and lack of proper training. [29], [30]. Hence, the proposed signal normalization scheme does not achieve a satisfactory force invariant EMG-PR performance when only a single training force is adopted. An amputee must be suitably trained to generate a repetitive MAP for every gesture under different force levels before using the myoelectric prosthetic hand. In this scenario, the proposed signal normalization scheme can likely provide satisfactory force invariant EMG-PR performance using only a single training force.

TABLE 5. P-values when the classifier is trained with single force level and tested with three force levels.

	Reference	Parameter	Case-A	Case-B	Case-C
LDA	Case-D	Accuracy	p<0.001	p<0.001	p<0.001
		Sensitivity	p<0.001	p<0.001	p<0.001
		Specificity	p<0.001	p<0.001	p<0.001
		Precision	p<0.001	p<0.001	p<0.001
		F1 Score	p<0.001	p<0.001	p<0.001
	Case-C	Accuracy	p<0.001	p<0.001	
		Sensitivity	p<0.001	p<0.001	
		Specificity	p<0.001	p<0.001	
		Precision	p<0.001	p<0.001	
		F1 Score	p<0.001	p<0.001	
	Case-B	Accuracy	0.001		
		Sensitivity	0.001		
		Specificity	0.002		
		Precision	0.015		
		F1 Score	p<0.001		
SVM	Case-D	Accuracy	p<0.001	p<0.001	0.001
		Sensitivity	p<0.001	p<0.001	0.001
		Specificity	p<0.001	p<0.001	p<0.001
		Precision	p<0.001	p<0.001	p<0.001
		F1 Score	p<0.001	p<0.001	0.001
	Case-C	Accuracy	p<0.001	p<0.001	
		Sensitivity	p<0.001	p<0.001	
		Specificity	p<0.001	p<0.001	
		Precision	p<0.001	p<0.001	
		F1 Score	p<0.001	p<0.001	
	Case-B	Accuracy	p<0.001		
		Sensitivity	p<0.001		
		Specificity	p<0.001		
		Precision	0.118		
		F1 Score	p<0.001		
KNN	Case-D	Accuracy	p<0.001	p<0.001	0.012
		Sensitivity	p<0.001	p<0.001	0.012
		Specificity	p<0.001	p<0.001	0.008
		Precision	p<0.001	p<0.001	0.002
		F1 Score	p<0.001	p<0.001	0.019
	Case-C	Accuracy	p<0.001	p<0.001	
		Sensitivity	p<0.001	p<0.001	
		Specificity	p<0.001	p<0.001	
		Precision	p<0.001	p<0.001	
		F1 Score	p<0.001	p<0.001	
	Case-B	Accuracy	0.003		
		Sensitivity	0.003		
		Specificity	0.004		
		Precision	0.139		
		F1 Score	p<0.001		

Furthermore, it is noted that the classifiers provide higher EMG-PR performance when they are trained with the medium force level (for a single training force) and low and high force levels (for two training forces). The likely reason is that the adjacent force level(s) is (are) highly correlated. In this case, it is preferable to select a training force level such that the other testing force levels are highly correlated.

Finally, we evaluate the proposed EMG signal normalization scheme offline. In future work, the real-time EMG-PR

TABLE 6. P-values when the classifier is trained with two force levels and tested with three force levels.

	Reference	Parameter	Case-A	Case-B	Case-C
LDA	Case-D	Accuracy	p<0.001	p<0.001	p<0.001
		Sensitivity	p<0.001	p<0.001	p<0.001
		Specificity	p<0.001	p<0.001	p<0.001
		Precision	p<0.001	p<0.001	p<0.001
		F1 Score	p<0.001	p<0.001	p<0.001
	Case-C	Accuracy	p<0.001	p<0.001	
		Sensitivity	p<0.001	p<0.001	
		Specificity	p<0.001	p<0.001	
		Precision	p<0.001	p<0.001	
		F1 Score	p<0.001	p<0.001	
	Case-B	Accuracy	p<0.001		
		Sensitivity	p<0.001		
		Specificity	p<0.001		
		Precision	p<0.001		
		F1 Score	p<0.001		
SVM	Case-D	Accuracy	p<0.001	p<0.001	p<0.001
		Sensitivity	p<0.001	p<0.001	p<0.001
		Specificity	p<0.001	p<0.001	p<0.001
		Precision	p<0.001	p<0.001	p<0.001
		F1 Score	p<0.001	p<0.001	p<0.001
	Case-C	Accuracy	p<0.001	p<0.001	
		Sensitivity	p<0.001	p<0.001	
		Specificity	p<0.001	p<0.001	
		Precision	p<0.001	p<0.001	
		F1 Score	p<0.001	p<0.001	
	Case-B	Accuracy	p<0.001		
		Sensitivity	p<0.001		
		Specificity	p<0.001		
		Precision	0.003		
		F1 Score	p<0.001		
KNN	Case-D	Accuracy	p<0.001	p<0.001	p<0.001
		Sensitivity	p<0.001	p<0.001	p<0.001
		Specificity	p<0.001	p<0.001	p<0.001
		Precision	p<0.001	p<0.001	p<0.001
		F1 Score	p<0.001	p<0.001	p<0.001
	Case-C	Accuracy	p<0.001	p<0.001	
		Sensitivity	p<0.001	p<0.001	
		Specificity	p<0.001	p<0.001	
		Precision	p<0.001	p<0.001	
		F1 Score	p<0.001	p<0.001	
	Case-B	Accuracy	p<0.001		
		Sensitivity	p<0.001		
		Specificity	p<0.001		
		Precision	p<0.001		
		F1 Score	p<0.001		

TABLE 7. P-values when the classifier is trained and tested with three force levels.

	Reference	Parameter	Case-A	Case-B	Case-C
LDA	Case-D	Accuracy	p<0.001	p<0.001	0.003
		Sensitivity	p<0.001	p<0.001	0.003
		Specificity	p<0.001	p<0.001	0.002
		Precision	p<0.001	p<0.001	0.004
		F1 Score	p<0.001	p<0.001	0.003
	Case-C	Accuracy	0.002	0.006	
		Sensitivity	0.002	0.006	
		Specificity	0.003	0.008	
		Precision	0.002	0.007	
		F1 Score	0.002	0.006	
	Case-B	Accuracy	0.025		
		Sensitivity	0.025		
		Specificity	0.032		
		Precision	0.030		
		F1 Score	0.022		
SVM	Case-D	Accuracy	p<0.001	p<0.001	p<0.001
		Sensitivity	p<0.001	p<0.001	p<0.001
		Specificity	p<0.001	p<0.001	p<0.001
		Precision	p<0.001	p<0.001	p<0.001
		F1 Score	p<0.001	p<0.001	p<0.001
	Case-C	Accuracy	0.005	0.005	
		Sensitivity	0.005	0.005	
		Specificity	0.007	0.007	
		Precision	0.005	0.006	
		F1 Score	0.005	0.006	
	Case-B	Accuracy	0.090		
		Sensitivity	0.090		
		Specificity	0.094		
		Precision	0.097		
		F1 Score	0.089		
KNN	Case-D	Accuracy	p<0.001	p<0.001	0.004
		Sensitivity	p<0.001	p<0.001	0.004
		Specificity	p<0.001	p<0.001	0.004
		Precision	p<0.001	p<0.001	0.005
		F1 Score	p<0.001	p<0.001	0.005
	Case-C	Accuracy	0.004	0.017	
		Sensitivity	0.004	0.017	
		Specificity	0.005	0.016	
		Precision	0.004	0.019	
		F1 Score	0.004	0.017	
	Case-B	Accuracy	0.033		
		Sensitivity	0.033		
		Specificity	0.035		
		Precision	0.039		
		F1 Score	0.032		

performance of the proposed EMG signal normalization with nonlinearly transformed features (case D) can be studied to identify the robustness. In addition to the amplitude, the frequency-domain characteristics vary with the muscle force levels. Therefore, the frequency-domain characteristics should be considered in the future.

V. CONCLUSION

In this paper, we propose an EMG signal normalization scheme that is very helpful to balance the amplitude variation problem with muscle contraction forces. In addition to signal normalization, the nonlinear transformation of the features by the logarithm function helps in overlapping the MAP of different force levels and maximizing the margin among the gestures. Therefore, we establish a feature extraction method (case D) in which both the proposed signal normalization scheme and nonlinear transformation of the features are implemented. Compared to the considered recently reported models, the proposed feature extraction method helps significantly enhance the force invariant EMG-PR performance in terms of the accuracy, sensitivity, specificity, precision and F1 score. The experimental results also imply that the three classifiers provide almost identical EMG-PR performance, with the LDA classifier performing slightly better.

APPENDIX A

See Tables 5–8.

TABLE 8. The p-values between different feature extraction methods.

	Reference	Parameter	AR-RMS	TDF	Wavelet	TDPSD	TSD
LDA	Case-D	Accuracy	p<0.001	p<0.001	p<0.001	p<0.001	0.008
		Sensitivity	p<0.001	p<0.001	p<0.001	p<0.001	0.008
		Specificity	p<0.001	p<0.001	p<0.001	p<0.001	0.009
		Precision	p<0.001	0.001	p<0.001	0.002	0.008
		F1 Score	p<0.001	p<0.001	p<0.001	p<0.001	0.008
	TSD	Accuracy	0.006	0.010	0.012	0.103	
		Sensitivity	0.006	0.010	0.012	0.103	
		Specificity	0.005	0.010	0.011	0.089	
		Precision	0.005	0.010	0.008	0.103	
		F1 Score	0.006	0.010	0.011	0.091	
	TDPSD	Accuracy	0.004	0.003	0.022		
		Sensitivity	0.004	0.003	0.022		
		Specificity	0.003	0.004	0.015		
		Precision	0.003	0.003	0.013		
		F1 Score	0.004	0.003	0.024		
	Wavelet	Accuracy	0.020	0.022			
		Sensitivity	0.020	0.022			
		Specificity	0.018	0.022			
		Precision	0.025	0.027			
		F1 Score	0.020	0.020			
	TDF	Accuracy	0.446				
		Sensitivity	0.446				
		Specificity	0.440				
		Precision	0.430				
		F1 Score	0.420				
SVM	Case-D	Accuracy	p<0.001	0.001	p<0.001	0.002	0.009
		Sensitivity	p<0.001	0.001	p<0.001	0.002	0.009
		Specificity	p<0.001	0.001	p<0.001	0.002	0.007
		Precision	p<0.001	p<0.001	p<0.001	0.002	0.008
		F1 Score	p<0.001	0.001	p<0.001	0.002	0.010
	TSD	Accuracy	0.005	0.013	0.008	0.161	
		Sensitivity	0.005	0.013	0.008	0.161	
		Specificity	0.004	0.012	0.007	0.145	
		Precision	0.004	0.011	0.007	0.157	
		F1 Score	0.005	0.013	0.008	0.157	
	TDPSD	Accuracy	p<0.001	0.002	0.003		
		Sensitivity	p<0.001	0.002	0.003		
		Specificity	p<0.001	0.002	0.002		
		Precision	p<0.001	0.002	0.002		
		F1 Score	0.001	0.002	0.003		
	Wavelet	Accuracy	0.033	0.068			
		Sensitivity	0.033	0.068			
		Specificity	0.032	0.063			
		Precision	0.038	0.070			
		F1 Score	0.036	0.065			
	TDF	Accuracy	0.544				
		Sensitivity	0.544				
		Specificity	0.514				
		Precision	0.554				
		F1 Score	0.523				
KNN	Case-D	Accuracy	p<0.001	p<0.001	p<0.001	0.003	0.001
		Sensitivity	p<0.001	p<0.001	p<0.001	0.003	0.001
		Specificity	p<0.001	0.001	p<0.001	0.002	p<0.001
		Precision	p<0.001	p<0.001	p<0.001	0.003	0.001
		F1 Score	p<0.001	p<0.001	p<0.001	0.002	0.001
	TSD	Accuracy	0.003	0.010	0.005	0.148	
		Sensitivity	0.003	0.010	0.005	0.148	
		Specificity	0.002	0.009	0.005	0.134	
		Precision	0.002	0.009	0.004	0.149	
		F1 Score	0.003	0.010	0.005	0.140	
	TDPSD	Accuracy	p<0.001	0.002	0.006		
		Sensitivity	p<0.001	0.002	0.006		
		Specificity	p<0.001	0.002	0.004		
		Precision	p<0.001	0.002	0.004		
		F1 Score	p<0.001	0.002	0.006		
	Wavelet	Accuracy	0.011	0.051			
		Sensitivity	0.011	0.051			
		Specificity	0.011	0.045			
		Precision	0.010	0.056			
		F1 Score	0.011	0.049			
	TDF	Accuracy	0.825				
		Sensitivity	0.825				
		Specificity	0.766				
		Precision	0.847				
		F1 Score	0.807				

ACKNOWLEDGMENT

The authors would like to show sincere gratitude to Dr. Ali H. Al-Timemy and Dr. Rami N. Khushaba for making the EMG dataset publicly available on the website of Dr. Rami N. Khushaba. The dataset is available at https://www.rami-khushaba.com/electromyogram-emg-repository.html.

REFERENCES

[1] C. L. Ng and M. B. I. Reaz, "Evolution of a capacitive electromyography contactless biosensor: Design and modelling techniques," *Measurement*, vol. 145, pp. 460–471, Oct. 2019.

[2] C. L. Ng and M. B. I. Reaz, "Impact of skin-electrode capacitance on the performance of CEMG biosensor," *IEEE Sensors J.*, vol. 17, no. 9, pp. 2636–2637, May 2017.

[3] C. L. Ng, M. B. I. Reaz, and M. E. H. Chowdhury, "A low noise capacitive electromyography monitoring system for remote healthcare applications," *IEEE Sensors J.*, vol. 20, no. 6, pp. 3333–3342, Mar. 2020.

[4] X. Jiang, L.-K. Merhi, Z. G. Xiao, and C. Menon, "Exploration of force myography and surface electromyography in hand gesture classification," *Med. Eng. Phys.*, vol. 41, pp. 63–73, Mar. 2017.

[5] Z. G. Xiao and C. Menon, "A review of force myography research and development," *Sensors*, vol. 19, no. 20, p. 4557, Oct. 2019.

[6] H. Ashraf, A. Waris, M. Jamil, S. O. Gilani, I. K. Niazi, E. N. Kamavuako, and S. H. N. Gilani, "Determination of optimum segmentation schemes for pattern recognition-based myoelectric control: A multi-dataset investigation," *IEEE Access*, vol. 8, pp. 90862–90877, 2020.

[7] R. Chowdhury, M. Reaz, M. Ali, A. Bakar, K. Chellappan, and T. Chang, "Surface electromyography signal processing and classification techniques," *Sensors*, vol. 13, no. 9, pp. 12431–12466, Sep. 2013.

[8] M. B. I. Reaz, M. S. Hussain, and F. Mohd-Yasin, "Techniques of EMG signal analysis: Detection, processing, classification and applications," *Biol. Procedures Online*, vol. 8, no. 1, pp. 11–35, Dec. 2006.

[9] A. Jaramillo-Yánez, M. E. Benalcázar, and E. Mena-Maldonado, "Real-time hand gesture recognition using surface electromyography and machine learning: A systematic literature review," *Sensors*, vol. 20, no. 9, pp. 1–36, Jan. 2020.

[10] A. H. Al-Timemy, R. N. Khushaba, G. Bugmann, and J. Escudero, "Improving the performance against force variation of EMG controlled multifunctional upper-limb prostheses for transradial amputees," *IEEE Trans. Neural Syst. Rehabil. Eng.*, vol. 24, no. 6, pp. 650–661, Jun. 2016.

[11] J. He, D. Zhang, X. Sheng, S. Li, and X. Zhu, "Invariant surface EMG feature against varying contraction level for myoelectric control based on muscle coordination," *IEEE J. Biomed. Health Informat.*, vol. 19, no. 3, pp. 874–882, May 2015.

[12] F. Onay and A. Mert, "Phasor represented EMG feature extraction against varying contraction level of prosthetic control," *Biomed. Signal Process. Control*, vol. 59, May 2020, Art. no. 101881.

[13] M. G. Asogbon, O. W. Samuel, Y. Geng, O. Oluwagbemi, J. Ning, S. Chen, N. Ganesh, P. Feng, and G. Li, "Towards resolving the co-existing impacts of multiple dynamic factors on the performance of EMG-pattern recognition based prostheses," *Comput. Methods Programs Biomed.*, vol. 184, Feb. 2020, Art. no. 105278.

[14] R. Hu, X. Chen, X. Zhang, and X. Chen, "Adaptive electrode calibration method based on muscle core activation regions and its application in myoelectric pattern recognition," *IEEE Trans. Neural Syst. Rehabil. Eng.*, vol. 29, pp. 11–20, 2021.

[15] A. J. Young, L. J. Hargrove, and T. A. Kuiken, "Improving myoelectric pattern recognition robustness to electrode shift by changing interelectrode distance and electrode configuration," *IEEE Trans. Biomed. Eng.*, vol. 59, no. 3, pp. 645–652, Mar. 2012.

[16] J. He, X. Sheng, X. Zhu, and N. Jiang, "Position identification for robust myoelectric control against electrode shift," *IEEE Trans. Neural Syst. Rehabil. Eng.*, vol. 28, no. 12, pp. 3121–3128, Dec. 2020.

[17] A. Fougner, E. Scheme, A. D. C. Chan, K. Englehart, and Ø. Stavdahl, "Resolving the limb position effect in myoelectric pattern recognition," *IEEE Trans. Neural Syst. Rehabil. Eng.*, vol. 19, no. 6, pp. 644–651, Dec. 2011.

[18] R. N. Khushaba, A. Al-Timemy, S. Kodagoda, and K. Nazarpour, "Combined influence of forearm orientation and muscular contraction on EMG pattern recognition," *Expert Syst. Appl.*, vol. 61, pp. 154–161, Nov. 2016.

[19] A. K. Mukhopadhyay and S. Samui, "An experimental study on upper limb position invariant EMG signal classification based on deep neural network," *Biomed. Signal Process. Control*, vol. 55, Jan. 2020, Art. no. 101669.

[20] E. Campbell, A. Phinyomark, and E. Scheme, "Current trends and confounding factors in myoelectric control: Limb position and contraction intensity," *Sensors*, vol. 20, no. 6, p. 1613, Mar. 2020.

[21] T. Lorrain, N. Jiang, and D. Farina, "Influence of the training set on the accuracy of surface EMG classification in dynamic contractions for the control of multifunction prostheses," *J. NeuroEng. Rehabil.*, vol. 8, no. 1, p. 25, 2011.

[22] T. W. Calvert and A. E. Chapman, "The relationship between the surface EMG and force transients in muscle: Simulation and experimental studies," *Proc. IEEE*, vol. 65, no. 5, pp. 682–689, May 1977.

[23] A. L. Hof, "The relationship between electromyogram and muscle force," *Sportverletzung-Sportschaden*, vol. 11, no. 3, pp. 79–86, Sep. 1997.

[24] E. Shwedyk, R. Balasubramanian, and R. N. Scott, "A nonstationary model for the electromyogram," *IEEE Trans. Biomed. Eng.*, vol. BME-24, no. 5, pp. 417–424, Sep. 1977.

[25] D. Tkach, H. Huang, and T. A. Kuiken, "Study of stability of time-domain features for electromyographic pattern recognition," *J. Neuroeng. Rehabil.*, vol. 7, no. 1, pp. 1–13, Dec. 2010.

[26] E. Scheme and K. Englehart, "Electromyogram pattern recognition for control of powered upper-limb prostheses: State of the art and challenges for clinical use," *J Rehabil. Res. Develop.*, vol. 48, no. 6, pp. 643–660, 2011.

[27] S. Hua, C. Wang, Z. Xie, and X. Wu, "A force levels and gestures integrated multi-task strategy for neural decoding," *Complex Intell. Syst.*, vol. 6, no. 3, pp. 469–478, Oct. 2020.

[28] A. Ameri, M. A. Akhaee, E. Scheme, and K. Englehart, "A deep transfer learning approach to reducing the effect of electrode shift in EMG pattern recognition-based control," *IEEE Trans. Neural Syst. Rehabil. Eng.*, vol. 28, no. 2, pp. 370–379, Feb. 2020.

[29] Z. Zhu, C. Martinez-Luna, J. Li, B. E. McDonald, C. Dai, X. Huang, T. R. Farrell, and E. A. Clancy, "EMG-force and EMG-target models during force-varying bilateral hand-wrist contraction in able-bodied and limb-absent subjects," *IEEE Trans. Neural Syst. Rehabil. Eng.*, vol. 28, no. 12, pp. 3040–3050, Dec. 2020.

[30] L. Pan, D. Zhang, X. Sheng, and X. Zhu, "Improving myoelectric control for amputees through transcranial direct current stimulation," *IEEE Trans. Biomed. Eng.*, vol. 62, no. 8, pp. 1927–1936, Aug. 2015.

[31] R. N. Khushaba, A. H. Al-Timemy, A. Al-Ani, and A. Al-Jumaily, "A framework of temporal-spatial descriptors-based feature extraction for improved myoelectric pattern recognition," *IEEE Trans. Neural Syst. Rehabil. Eng.*, vol. 25, no. 10, pp. 1821–1831, Oct. 2017.

[32] L. I. B. López, Á. L. V. Caraguay, V. H. Vimos, J. A. Zea, J. P. Vásconez, M. Álvarez, and M. E. Benalcázar, "An energy-based method for orientation correction of EMG bracelet sensors in hand gesture recognition systems," *Sensors*, vol. 20, no. 21, pp. 1–34, Jan. 2020.

[33] D. C. Toledo-Perez, J. Rodriguez-Resendiz, and R. A. Gomez-Loenzo, "A study of computing zero crossing methods and an improved proposal for EMG signals," *IEEE Access*, vol. 8, pp. 8783–8790, 2020.

[34] B. Hudgins, P. Parker, and R. N. Scott, "A new strategy for multifunction myoelectric control," *IEEE Trans. Biomed. Eng.*, vol. 40, no. 1, pp. 82–94, Jan. 1993.

[35] B. Hjorth, "EEG analysis based on time domain properties," *Electroencephalogr. Clin. Neurophysiol.*, vol. 29, no. 3, pp. 306–310, Sep. 1970.

[36] X. Chen, X. Zhu, and D. Zhang, "A discriminant bispectrum feature for surface electromyogram signal classification," *Med. Eng. Phys.*, vol. 32, no. 2, pp. 126–135, Mar. 2010.

[37] T. R. Farrell and R. F. Weir, "The optimal controller delay for myoelectric prostheses," *IEEE Trans. Neural Syst. Rehabil. Eng.*, vol. 15, no. 1, pp. 111–118, Mar. 2007.

[38] C. J. De Luca, L. D. Gilmore, M. Kuznetsov, and S. H. Roy, "Filtering the surface EMG signal: Movement artifact and baseline noise contamination," *J. Biomech.*, vol. 43, no. 8, pp. 1573–1579, May 2010.

[39] M. Simao, N. Mendes, O. Gibaru, and P. Neto, "A review on electromyography decoding and pattern recognition for human-machine interaction," *IEEE Access*, vol. 7, pp. 39564–39582, 2019.

[40] S. Yacoub and K. Raoof, "Power line interference rejection from surface electromyography signal using an adaptive algorithm," *IRBM*, vol. 29, no. 4, pp. 231–238, Sep. 2008.

[41] D. Cai, X. He, and J. Han, "SRDA: An efficient algorithm for large-scale discriminant analysis," *IEEE Trans. Knowl. Data Eng.*, vol. 20, no. 1, pp. 1–12, Jan. 2008.
[42] L. Pan, D. Zhang, J. Liu, X. Sheng, and X. Zhu, "Continuous estimation of finger joint angles under different static wrist motions from surface EMG signals," *Biomed. Signal Process. Control*, vol. 14, pp. 265–271, Nov. 2014.
[43] A. H. Al-Timemy, G. Bugmann, J. Escudero, and N. Outram, "Classification of finger movements for the dexterous hand prosthesis control with surface electromyography," *IEEE J. Biomed. Health Informat.*, vol. 17, no. 3, pp. 608–618, May 2013.
[44] T. Matsubara and J. Morimoto, "Bilinear modeling of EMG signals to extract user-independent features for multiuser myoelectric interface," *IEEE Trans. Biomed. Eng.*, vol. 60, no. 8, pp. 2205–2213, Aug. 2013.
[45] R. N. Khushaba, M. Takruri, J. V. Miro, and S. Kodagoda, "Towards limb position invariant myoelectric pattern recognition using time-dependent spectral features," *Neural Netw.*, vol. 55, pp. 42–58, Jul. 2014.
[46] R. N. Khushaba, S. Kodagoda, M. Takruri, and G. Dissanayake, "Toward improved control of prosthetic fingers using surface electromyogram (EMG) signals," *Expert Syst. Appl.*, vol. 39, no. 12, pp. 10731–10738, Sep. 2012.
[47] P. Banerjee, F. O. Dehnbostel, and R. Preissner, "Prediction is a balancing act: Importance of sampling methods to balance sensitivity and specificity of predictive models based on imbalanced chemical data sets," *Frontiers Chem.*, vol. 6, pp. 1–11, Aug. 2018.
[48] O. W. Samuel, M. G. Asogbon, Y. Geng, N. Jiang, D. Mzurikwao, Y. Zheng, K. K. L. Wong, L. Vollero, and G. Li, "Decoding movement intent patterns based on spatiotemporal and adaptive filtering method towards active motor training in stroke rehabilitation systems," *Neural Comput. Appl.*, vol. 33, no. 10, pp. 4793–4806, Jan. 2021.
[49] E. C. Wentink, E. C. Prinsen, J. S. Rietman, and P. H. Veltink, "Comparison of muscle activity patterns of transfemoral amputees and control subjects during walking," *J. NeuroEng. Rehabil.*, vol. 10, no. 1, p. 87, 2013.
[50] R. N. Khushaba, S. Kodagoda, S. Lal, and G. Dissanayake, "Driver drowsiness classification using fuzzy wavelet-packet-based feature-extraction algorithm," *IEEE Trans. Biomed. Eng.*, vol. 58, no. 1, pp. 121–131, Jan. 2011.
[51] Y.-C. Du, C.-H. Lin, L.-Y. Shyu, and T. Chen, "Portable hand motion classifier for multi-channel surface electromyography recognition using grey relational analysis," *Expert Syst. Appl.*, vol. 37, no. 6, pp. 4283–4291, Jun. 2010.
[52] Y. Huang, K. B. Englehart, B. Hudgins, and A. D. C. Chan, "A Gaussian mixture model based classification scheme for myoelectric control of powered upper limb prostheses," *IEEE Trans. Biomed. Eng.*, vol. 52, no. 11, pp. 1801–1811, Nov. 2005.
[53] N. V. Iqbal, K. Subramaniam, and S. Asmi P, "Robust feature sets for contraction level invariant control of upper limb myoelectric prosthesis," *Biomed. Signal Process. Control*, vol. 51, pp. 90–96, May 2019.

MD. JOHIRUL ISLAM received the B.Sc. and M.Sc. degrees in applied physics and electronic engineering from the University of Rajshahi, Rajshahi, Bangladesh, in 2011 and 2012, respectively. He is currently an Assistant Professor with the Department of Physics, Rajshahi University of Engineering and Technology, Rajshahi. He is also a Ph.D. Research Fellow with the Department of Electrical and Electronic Engineering, University of Rajshahi. His research interests include human–machine interfacing, biomedical instrumentation, and embedded systems.

SHAMIM AHMAD (Member, IEEE) received the B.Sc. and M.Sc. degrees in applied physics and electronic engineering from the University of Rajshahi, Rajshahi, Bangladesh, and the Doctor of Engineering degree in electrical engineering from Chubu University, Japan. Following that, he worked as a Post-Graduate Research Student with the Department of Computer Engineering, Inha University, South Korea. He is currently working as a Professor with the Department of Computer Science and Engineering, University of Rajshah. His area of research interests include bioinformatics, embedded systems, and image processing.

FAHMIDA HAQUE received the B.Sc. degree in electrical and electronic engineering from American International University-Bangladesh. She is currently pursuing the Ph.D. degree with the Department of Electrical, Electronic and System Engineering, Universiti Kebangsaan Malaysia, Bangi, Malaysia. Her area of research interests include electronics, biomedical systems, biomedical signal processing, and machine learning.

MAMUN BIN IBNE REAZ (Senior Member, IEEE) was born in Bangladesh, in December 1963. He received the B.Sc. and M.Sc. degrees in applied physics and electronics from the University of Rajshahi, Bangladesh, in 1985 and 1986, respectively, and the D.Eng. degree from Ibaraki University, Japan, in 2007. He has been a Senior Associate with the Abdus Salam International Centre for Theoretical Physics (ICTP), Italy, since 2008. He is currently a Professor with the Department of Electrical, Electronic and Systems Engineering, Faculty of Engineering and Built Environment, Universiti Kebangsaan Malaysia, Malaysia, involving in teaching, research, and industrial consultation. He has vast research experiences in Japan, Italy, and Malaysia. He has published extensively in the area of IC design, biomedical application IC, and smart home. He is author and coauthor of more than 300 research articles in design automation and IC design for biomedical.

MOHAMMAD A. S. BHUIYAN was born in Chittagong, Bangladesh, in 1985. He received the B.Sc. and M.Sc. degrees in applied physics, electronics and communication engineering from the University of Chittagong, Bangladesh, in 2006 and 2007, respectively, and the Ph.D. degree from Universiti Kebangsaan Malaysia, Malaysia, in 2017. He is currently an Assistant Professor with the Department of Electrical and Electronics Engineering, Xiamen University Malaysia, Malaysia. He has over ten years of active teaching and research experience and authored over 70 indexed international journal and conference papers with a citation count of over 450 and an H-index of 13. His current research interests include VLSI and wireless communication.

MD. REZAUL ISLAM received the B.Sc. and M.Sc. degrees in applied physics and electronics from the University of Rajshahi, Rajshahi, Bangladesh, in 1982 and 1983, respectively. He is currently a Professor with the Department of Electrical and Electronic Engineering, University of Rajshahi. His area of research interests include electronics, biomedical instrumentation, biomedical signal processing, and embedded systems.